MICROSTRUCTURAL FEATURES OF VOLCANIC AEROSOLS

L.S. Ivlev

Institute of Physics at the St. Petersburg State University
Received April 9, 1996

A conclusion that the particle size distribution patterns are governed by volcanic activity has been drawn based on the volcanic aerosol dispersity data analysis. The maximums of the distribution function have been found in the diameter ranges of particle size 2–4 μm, 0.6–0.9 μm, and d > 0.5 μm. Particles with size 0.6–0.9 μm are supposed to be responsible for the anomalous spectral behavior of the aerosol extinction. Regularities in the enrichment factor behavior of some chemical elements in volcanic aerosols have been discovered to be determined by the eruption intensity, time elapsed from the start of emission, and distance of an aerosol sampling site from a volcanic crater. In particular, the enrichment factor for S *has been found to increase with time. The increase of the enrichment factor for a number of volatile metals with altitude has been found.*

1. INTRODUCTION

Three powerful volcanic eruptions (of Saint Helens, El-Chichon, and Pinatubo volcanos) occurred since 1980 forced some re-estimations of the contribution of volcanic products to the pollution of the troposphere and stratosphere and of their role in radiative and climatic processes to be made. Whereas the leading role of volcanic eruptions in the formation of the stratospheric aerosol layer has been already supposed to be obvious,[1,2] recent results of experimental investigations[3–5] are evidence of their noticeable contribution to the content of the tropospheric aerosol and sulfur gas. Since the lifetime of sulfur gas in the troposphere is significantly longer than in the stratosphere, one can suppose that from the troposphere it penetrates the stratosphere long after eruption and generates there the sulfuric acid and sulfate particles with size $r \leq 0.2$ μm.

Volcanic dispersed aerosols with size $r \leq 1$ μm in the dry cloudless troposphere exist significantly longer ($\tau^t_{volc} \approx 50$ days) than it is supposed for the majority of tropospheric aerosol models[6–8] ($\tau^t_{aer} \approx 10$ days). Since long cloudless periods are observed at low latitudes, it is obvious that aerosol substance from even weak volcanic eruptions is accumulated in the troposphere during this time. The portion of the primordial volcanic aerosol at higher latitudes is noticeable only in the upper troposphere above the basic cloud layer ($z \geq 5$ km).

One can expect the manifestation of the contribution of primordial volcanic aerosols, for example, through the optical properties of the atmosphere, in particular, through the spectral behavior of the atmospheric optical thickness under condition of low turbidity of the ground layer when the stratospheric layer of the sulfate aerosols is not

very dense. The second condition is satisfied either just after powerful volcanic eruption, or without penetration of the volcanic matter to the stratosphere. At the same time, the significant pollution of the ground layer by particles enriched with the elements dangerous to health (Pb, Hg, Zn, Cr, Cd, etc.) is observed near the volcano. These aerosols have also high catalytic and photocatalytic activity, in particular, they quicken decomposition of ozone molecules in the lower atmospheric layers.[9,10]

The estimates of the role of the primordial volcanic aerosols in the processes listed above are inaccurate and, perhaps, underestimated. To refine such estimates, it is necessary to reveal the characteristic peculiarities of microstructure of these aerosols, their elemental and chemical composition, and possible manifestations through the optical properties of the tropospheric aerosols.

2. SIZE DISTRIBUTION OF VOLCANIC DUST PARTICLES

There are relatively few direct measurements of the size distribution of particles of volcanic origin.[11–13] High concentration of giant particles ($r > 1$ μm) and their strong spatiotemporal variability are observed.

Measurements of aerosols in the ground atmospheric layer near active volcanos of Kamchatka (Tolbachik, Klyuchevskoi, Gorelyi, Karymskii, and Mutnovskii) were carried out repeatedly by researchers of the Aerosol Laboratory of the Scientific-Research Institute of Physics at the St. Petersburg State University in 1974–1981. The particle size distribution in the range of particle size $r \geq 0.2$ μm was measured with the AZ–5M photoelectric counter and determined by means of an electron microscopic analysis of impactor and filter aerosol samples[12] for $r \leq 0.5$ μm.

Quite large data arrays $\Delta N(r \geq 0.2)$ were obtained under different meteorological conditions for different intensities of volcanic substance emission. Analogous measurements were carried out in 1994–1995 in Mexico near Colima, Paracutin, and Popocatepetl volcanos. Aerosol measurements were carried out during the Mt. Popocatepetl eruption (from December 21, 1994 to January 28, 1995) by means of the AZ–5M photoelectric counter from onboard the aircraft and the ashfalls were studied.[14] The most difficult problem in obtaining the size spectra of particles of volcanic origin was separation of this spectrum from the data obtained when measuring relatively weak eruption of volcanic substance and far from the volcanic crater.

When measuring in Kamchatka, one can suppose that only background aerosol particles are additionally present in the ground atmospheric layer, but when measuring in Mexico, one should take into account a strong effect of the soil in the dry season as well as the presence of products of vegetation (sugar-cane) burning and anthropogenic pollution. The data were averaged over several days for different times of the day and the contribution of aerosols of non-volcanic origin was subtracted, where possible.

The possibilities of selection of aerosols of different origin are most clear when using the function $\Delta V(r)$ or $\Delta V(r)/\Delta r$. Generation and evolution of modes with different r_0 occur in different ways, which is why the modes can be identified. In particular, such an approach gave good results when measuring the aerosols of Mt. Paracutin. The measurements were carried out near the volcano at different distances from it and on the other side from Mt. Tansitaro (in Apo) being higher than Mt. Paracutin. The measurements were carried out under conditions of low continuous cloudiness and daily rains in the evening.

The results of subtracting the background values of $\Delta V(r)/\Delta r$ from the function $\Delta V(r)/\Delta r$ are shown in Fig. 1 for measurements at three sites (*1* is for Apo, *2* is for a field 16 km apart from the volcano, and *3* is for the foot of the volcano approximately 6 km apart from the crater). The particles of volcanic origin are well pronounced in the ranges of particle size $0.5 \leq d \leq 0.9$ μm and $1.5 \leq d \leq 7.0$ μm. The negative value $\Delta_i (\Delta V/\Delta r)$ was observed in the range $2.0 \leq d \leq 7$ μm for measurements at the site 16 km apart from the volcanic crater and in the range of particle size $0.4 \leq d \leq 0.8$ μm for measurements in Apo. This is evidence of the additional contribution of volcanic particles of these size ranges to the so-called "background" particle size distribution function, i.e., the true size distribution of the particles of volcanic origin should have still better pronounced maximums of the distribution in these size ranges. When measuring the concentration and dispersity of dust particles after the eruption of Colima volcano, the three-day series of measurements was carried out just under the crater of Fuego De Colima volcano in the Plion valley blinded by the tops of Mts. Fuego, Nevada, and

Volcansito at an altitude of 3500 m. One can take these data as most representative of the conditions of measuring immediately volcanic aerosols for weak aerosol emission (Fig. 2).
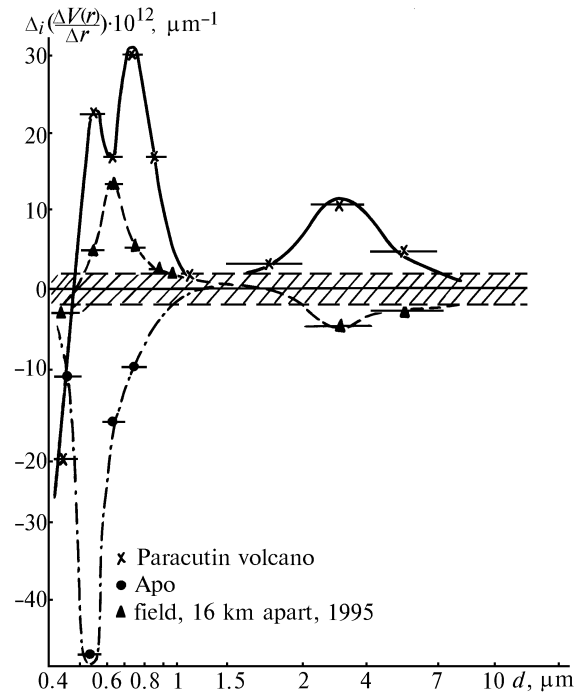

FIG. 1. *Average differences between volume particle size distribution functions at different points in the vicinity of Paracutin volcano and the "background" distribution measured on July 13–16, 1995.*
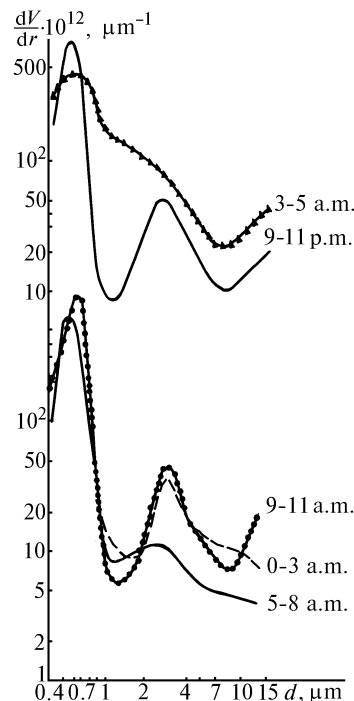

FIG. 2. *Average volume particle size distribution functions in the Plion valley under the crater of Fuego de Colima volcano at different times of the day on May 9–11, 1995.*

The diurnal transformation of the particle size spectrum caused by both meteorological conditions and additional dusting from the volcanic slope surface is well pronounced in the three-day average data. (Secondary raising of the settled volcanic dust.) The number density of aerosols of volcanic origin was deliberately higher than the background one in measurements carried out near Karymskii and Popocatepetl volcanos; however, the particles with different lifetimes before the start of measurements were mixed in these cases. This slightly smeared the size spectra of particles emitted from the crater in different regimes of volcanic substance emission.

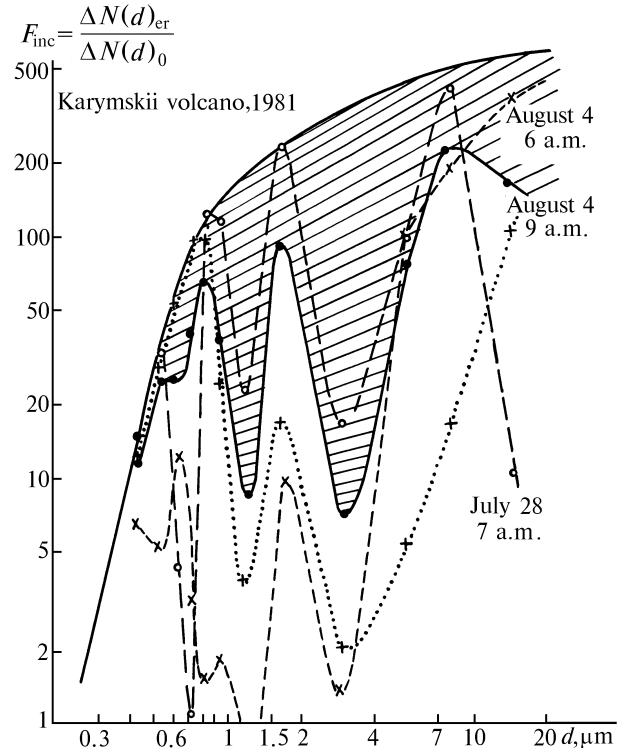$$F_{inc} = \frac{\Delta N(d)_{er}}{\Delta N(d)_0}$$

FIG. 3. Ratios of number densities of particles of different size during the intense emission of Karymskii volcano to that measured without emission (before the eruption).

Three strong emissions of volcanic dust were observed when measuring near Karymskii volcano in 1981: on July 28 at 6–8 a.m. and on August 4 at 6–7 and 9–10 a.m. The factors of increasing $F_{inc} = \Delta N_i / \Delta N_0$ of the number density of particles of different size in comparison with the background one were calculated (Fig. 3). The difference between the envelope and the mean experimental value of F_{inc} is evidence of the fact that accumulation of particles with size $0.5 \leq d \leq 0.8$ µm, $0.9 \leq d \leq 1.5$ µm and $2.0 \leq d \leq 7.0$ µm and, perhaps, $d \geq 10$ µm occurs in the ground layer during weak but permanent emission of volcanic dust into the atmosphere. (The error in determining the background number density of the particles with size $d \geq 10$ µm is very large.)

We note that the function dV/dr obtained for the particles emitted from Popocatepetl volcano crater during the most powerful emissions has relatively weakly pronounced polymodality (Fig. 4). The polymodality of

the structure of dust particles becomes better pronounced as the emission weakens (Fig. 5).
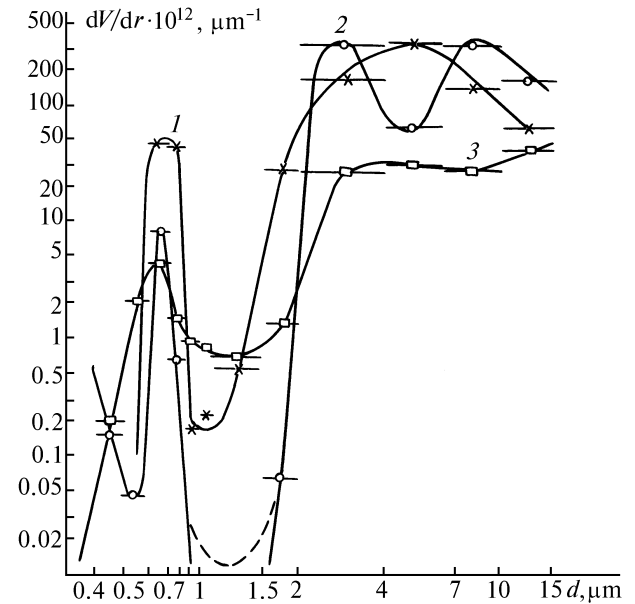

FIG. 4. Volume particle size distribution functions during very powerful emissions of aerosol matter by Popocatepetl volcano (December 27, 1994): 1) plume boundary, 2) center, 3) out of the plume.
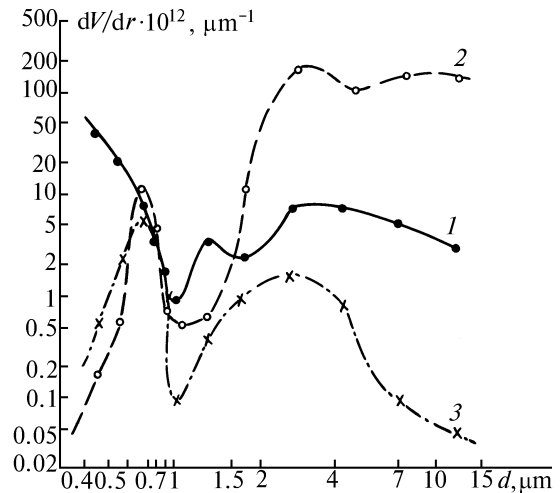
FIG. 5. Volume particle size distribution functions during relatively weak emission of aerosol matter by Popocatepetl volcano (plume center); 1) December 29, 1994; 2) January 6, 1995; 3) January 21, 1995.

The contribution of volcanic dust to the total content of aerosols of the ground layer relatively far from the crater is of undoubted interest. In this case, one can estimate the effective strength of the source of particles, assuming the stationarity of the particle flux: $mv(x) = $ const. It is possible when comparing the data on dispersity and number density of particles in dry and wet seasons, assuming that the source acts continuously. Measurements were carried out at the Refuhio ranch, approximately 20 km apart from

the Colima volcano crater. Average distribution functions $\Delta N(d)$, in cm^{-3}, were calculated for both seasons. Diurnal variability of the aerosol dispersity was the governing factor in all cases both in dry and wet seasons. However, the bulk of the data array for the wet season was obtained only at 11−12 a.m. So different variants of the $\Delta N'(d)$ were calculated for the dry season: 1) for the period 11−12 a.m.; 2) daily average; 3) mean values between these two cases (Table I).

TABLE I. *Characteristic size distribution functions of aerosol particles* $\Delta N(d)$, l^{-1} *near the volcanos for different intensities of emission of the matter.*

$\Delta d(>)$, μm	Kluchevskoi volcano (Steller fumarole) August 1974	Gorelyi volcano July−August 1980	Karymskii volcano July−August 1981		Fuego de Colima volcano December 1994	Fuego de Colima volcano May 1995
0.01	8000	7000	9000	8000	−	10000
0.02	18000	12000	16000	18000	−	17000
0.03	32800	31000	28000	35000	−	37000
0.05	40000	37000	32000	42000	−	70000
0.10	36000	34000	33000	40000	−	50000
0.20	32000	30000	27000	34000	−	35000
0.30	18800	6000	19000	31000	−	23000
0.40	7200	7000	7400	22000	6000	25400
0.50	1400	740	1944	14000	25500	30700
0.60	180	120	785	10000	64600	1430
0.70	60	91	264	4500	77000	3830
0.80	48	63	165	2000	42800	780
0.90	40	35	72.7	1750	35600	200
1.00	28	45	54.7	3500	17500	217
1.50	40	38	61.9	9000	2800	83
2.00	120	104	94.8	23000	330	118
4.00	16	1.86	30.7	19000	90	25.4
7.00	10	1.50	11.4	3000	21	5.0
10.00	5	1.90	6.70	500	10	3.35

TABLE I (*continued*).

$\Delta d(>)$, μm	Paracutin volcano July 1995	Popocatepetl volcano December 27, 1994	Popocatepetl volcano December 27−29, 1994	Popocatepetl volcano January 6, 1995	Popocatepetl volcano December 1994−January 1995
0.01	−	−	−	48000	30000
0.02	−	−	−	75000	63000
0.03	−	−	−	113000	110000
0.05	−	−	−	224000	150000
0.10	−	−	−	132000	80000
0.20	−	−	−	140000	45000
0.30	−	−	−	105000	8000
0.40	10600	4000	340	86000	1140
0.50	25800	1000	940	37800	3600
0.60	15200	600	30600	30000	16200
0.70	9100	900	19800	5940	5720
0.80	3280	1000	4160	510	5380
0.90	392	2400	4900	1400	12900
1.00	242	2000	2640	1540	15400
1.50	192	4200	4000	280	770
2.00	162	25000	12300	116	1200
4.00	39.8	16000	1360	5.46	97.5
7.00	2.35	3200	570	0.32	25.2
10.00	1.10	2300	300	0.05	6.12

N o t e :   Data in the range of particle size $d = 0.01-0.4$ μm are for individual impactor samples. Data for $d > 0.4$ μm are the data measured with the photoelectric counter, averaged over no less than 10 series for weak emissions and over 2−3 series for emissions with N (10) > 100 l^{-1}.

The curve of variation of the relative number density of particles of different size $E(d) = \Delta N_w / \Delta N_d$ and the average curve of possible washing-out of particles by precipitation[15] (envelope) obtained from these data are shown in Fig. 6. The difference between curves $\Delta N'(d)$ caused by continuous generation of particles in any variant of calculations remained practically constant. One can suppose that some portion of the aerosol is generated by the soil surface, in particular, after its quick heating and drying, in the range of particle size $d > 7$ μm. However, generation of particles with size $0.5 \le d \le 0.8$ μm can be explained only by increased emission of volcanic substance in a wet medium, which was visually observed.
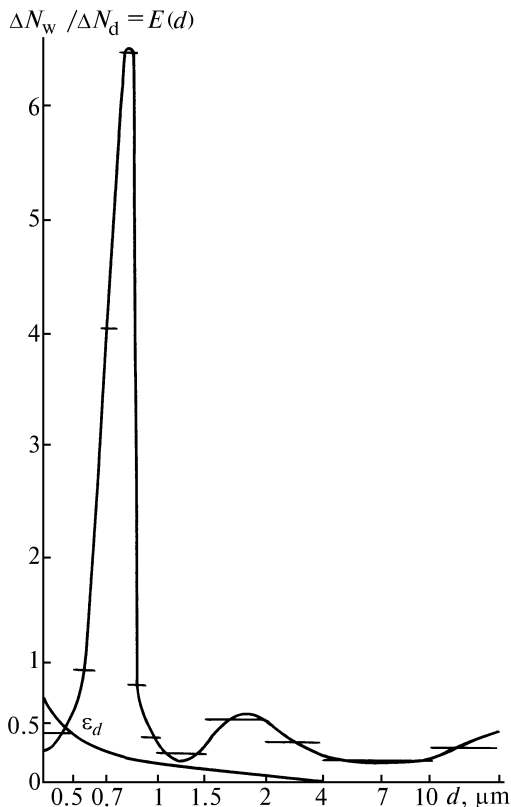

FIG. 6. *Average ratio of number densities of particles of different size at the wet season (July 1995) to that at the dry season (May 1995) for Colima volcano measured in Refuhio.*

Analogous calculations were done for aerosol measurements immediately near Colima, at the site approximately 45 km apart from the crater of the volcano (at the Center of Atmospheric Research of the University of Colima). Average data of May (dry season) and July (wet season) measurements from 10 a.m. to 1 p.m., when intense mixing of air mass is observed and heavy precipitation is practically absent, were taken for calculations. In this case more pronounced washing-out of particles from the atmosphere than at Refuhio site was observed for all measurable particle size ranges, except $0.9 \le d \le 1.0$ μm (Fig. 7).
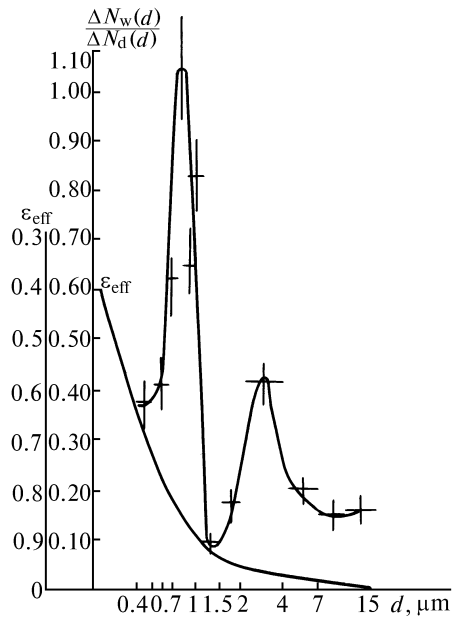

FIG. 7. *Washing-out of particles of different size by precipitation according to measurements in Colima (at the Center of Atmospheric Research in May–July, 1995).*

According to these data, one can suppose that continuous generation of aerosol particles occurs in two particle size ranges, namely, $0.5 \le d \le 1.0$ μm and $2.0 \le d \le 7.0$ μm, i.e., approximately in the same ranges as for Refuhio.

The average data on particles size distribution function dN/dr are given in Table I for different volcanos. Some peculiarities of the particle size distribution functions are seen. The distribution cannot be described by a simple analytical expression even in the range of particle size $d \ge 0.4$ μm.

The polymodal structure of aerosols of volcanic origin is clearly manifested if we use the function $dV/dr = (4\pi/3)r^3 dN/dr$. The modes with $d < 7$ μm, $4 \ge d \ge 2$ μm, $0.9 \ge d > 0.6$ μm, and $d \le 0.5$ μm are observed in all cases. The relations among these modes change and the modal diameters are slightly shifted as functions of the emission intensity, meteorological conditions, and the distance between the measurement site and the volcano crater. The strongest variations of the function dV/dr vs. the intensity of emission are observed for the modes $0.9 \ge d \ge 0.6$ μm and $4 \ge d \ge 2$ μm. The mode $d \ge 7.0$ μm also can be caused by dusting from the soil and is not quite well pronounced in the case of weak emission of the volcanic substance. The mode with $4 \ge d \ge 2$ μm smears for strong eruption due to the sharp increase of the number of giant particles (see Fig. 2). The mode with $4 \ge d \ge 2$ μm is the stablest in the shape of the distribution curve.

It also should be noted that the increase of the particle number density in this range of particle size is best pronounced at the beginning of the sharp increase of the emission of volcanic substance, before increasing the number density of particles with size $0.9 \ge d \ge 0.6$

and $d > 7.0$ μm. The extension of the particle size range, in which the maximums of the volume distribution dV/dr are observed for $d \geq 10$ μm and $d \leq 0.9$ μm, occurs due to explosive nature of the emission of volcanic substance. Especially large increase of the emitted particles with size $d \leq 0.9$ μm is sometimes observed in this case. The narrow sharply pronounced peaks that can be shifted from $d = 0.9$ μm to $d \leq 1.5$ μm and from $d \leq 0.5$ μm to $d \sim 0.6-0.7$ μm are observed in the particle size distribution function. These maximums disappear for long emission of decreasing intensity. So they are not observed practically when measuring far from the volcano crater.

The conglomerates of spherical aerosol particles with the mean size of about $1.5-2$ μm, which decompose after drying, were observed in thermal emission from the Popocatepetl volcano crater in January of 1995. The aerodynamics of such aggregates was considered in Ref. 16.

Table II presents the average model size distribution functions of volcanic dust particles obtained from the results of observations of the aerosols near the aforementioned volcanos, as well as according to data of other authors.[13,17-20]

It is supposed that the spectrum is modified due to sedimentation of particles with size larger than the threshold one.

TABLE II. *Model aerosol distributions, $\Delta N_i(d)$, cm^{-3}.*

Δd, μm	ΔN_1	$\Delta N_1'$	ΔN_2	$\Delta N_2'$	ΔN_3	$\Delta N_3'$
0.01−0.02	16.0	16.0	30.0	30.0	8.0	8.0
0.02−0.03	18.0	18.0	63.0	63.0	18.0	18.0
0.03−0.05	25.0	25.0	110.0	110.0	35.0	35.0
0.05−0.1	38.0	38.0	150.0	150.0	42.0	42.0
0.1−0.2	75.0	75.0	80.0	80.0	40.0	40.0
0.2−0.3	42.0	42.0	45.0	45.0	34.0	34.0
0.3−0.4	35.0	35.0	8.0	8.0	31.0	31.0
0.4−0.5	4.0	4.0	1.14	1.14	22.0	22.0
0.5−0.6	1.0	1.0	3.6	1.0	14.0	1.0
0.6−0.7	0.6	0.6	16.2	4.8	10.0	0.715
0.7−0.8	0.9	0.9	5.72	1.6	4.50	0.321
0.8−0.9	1.0	1.0	5.38	1.5	2.0	0.143
0.9−1.0	2.4	2.4	12.9	3.3	1.75	0.125
1.0−1.5	2.0	0.5	16.4	1.5	3.5	0.05
1.5−2.0	4.2	0.0	0.4	0.0	9.0	0.0
2.0−4.0	25.0	0.0	2.0	0.0	23.0	0.0
4.0−7.0	16.0	0.0	1.0	0.0	19.0	0.0
7.0−10.0	3.2	0.0	0.02	0.0	3.0	0.0
10.0−15.0	2.3	0.0	0.0	0.0	0.5	0.0

N o t e : $\Delta n_i(d)$ was obtained for $T = T_0$ and $\Delta N_i'(d)$ − for $T = T_0 + 30$ days.

3. MORPHOLOGICAL PROPERTIES OF PARTICLES

It is well known that the aerosols of volcanic origin are the particles of the finely dispersed lava, the products of abrasion of the crater walls, and the sulfuric acid droplets with the dissolved crystalline substance partly produced due to sublimation of magma.

Morphological structure of such particles is well known. The products of abrasion of the crater walls and the finely dispersed lava are similar to each other and are primarily the particles of irregular but quite simple shape with sharp edges. The particles of dispersed lava can contain microcavities and cleavages of round shape.

The microdroplets of sulfuric acid with crystalline patches are most characteristic of stratospheric aerosols.

In the troposphere, they are observed much more rarely.[22]

The electron microscopical analysis was carried out for individual samples collected by an impactor near the volcanos of Kamchatka and Mexico as well as in the Geyser valley of Kamchatka. The data on the morphological structure of particles of natural origin at another sites are presented in Table III for comparison. The number of the sulfuric acid droplets observed was insignificant for the majority of cases (Table III). However, their number sharply increased for samples collected in the Geyser valley and near fumaroles with weak emission. Their number becomes negligible with the increase of the particle size for $d > 0.2$ μm. This is evidence of the low rate of oxidation of the sulfur gas in the lower layers of the atmosphere even in the presence of metals−catalysts (Fe, Mn, Ti, Zn, Cr, etc.).

The relative number of the chain particles (fractals) is essentially different for the measurements in Mexico and Kamchatka. The noticeable decrease of the particles of this kind in Mexico was possibly related to the low relative humidity of air during collection of aerosol samples by the impactor and hence less degree of mechanical stability of aggregates.

Friable giant spheres of gray color with a diameter of 0.5−2 mm were visually observed during strong emissions ("puffs") of Popocatepetl volcano. These spheres decompose into small particles of irregular shape during the electron microscopical analysis. Obviously, these spherical aggregates were formed when the volcanic substance was released from the crater in a medium supersaturated by water vapor with very high number density of small dust particles. The ashfall in the vicinity of Popocatepetl volcano mainly consisted of these spheres. The study of the absorbability of ashes (Fig. 8) showed that it was low. Particles had low moisture-absorbing capacity. This is in agreement with low degree of mechanical stability of spherical aggregates at low relative humidity of the medium.
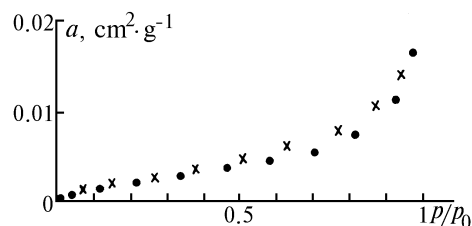

FIG. 8. *Adsorbability a, in* cm^2/g^{-1}, *of ashes of Popocatepetl volcano at different partial water vapor pressures* p/p_0 (*temperature* $T = 25°C$).

Previously, we investigated the effect of relative humidity on the morphological structure of natural aerosol particles in a fog chamber.[23] Table IV presents the distribution of particles over their types for three values of relative humidity: 23, 30, and 62%. A definite degree of correspondence is observed between the morphological structure of aerosols at a humidity of 62% and the volcanic aerosols of Kamchatka as well as between the morphological structure of aerosols when the relative humidity is in the range 23−30% and the volcanic aerosols of Mexico.

TABLE III. *Morphological structure of atmospheric aerosols.*

Site, time	Altitude above the surface, m	Particle types, %					
		Dense spheres	Low-dense spheres	Particles with coat	Dense nonspherical particles	Friable nonspherical particles	Chains
Ryl'sk, July−August 1975	0	10	16	10.3	46	15	2.7
	500	4.7	10.8	17.7	43.7	17.2	5.8
	2800	9.1	8.0	14.1	35.0	26.8	7.1
Bering Sea, August 1974	1000	18	65	1.5	8.0	−	7.5
	4000	41	30	12.8	2.5	10	3.7
	9000	12	40	11	15	9.0	13
Kamchatka, Steller fumarole, August 1974	1.5	3.3	15.7	7.9	16	35.6	21.5
Mutnovskii volcano, August 1980	1.5	8.0	12.0	5.5	21.5	40.0	13
Mexico, Popocatepetl volcano, January 1995	1.5	5.0	32	3.0	41	0	20
Colima volcano, May 1995	1.5	3.5	36	4.5	43	2.5	10.5

N o t e : The results of the electron microscopical analysis of individual impactor samples of the aerosol in the range of particle size from 0.02 to 0.8 μm.

TABLE IV. *Morphological structure of natural aerosols in the ground atmospheric layer as a function of the relative humidity* ($H = 2$ m, *August of 1980, Main Geophysical Observatory*).

Relative humidity, %	Particle types ($d = 0.02−0.8$ μm)					
	Dense spheres	Low-dense spheres	Particles with coat	Dense nonspherical particles	Low-dense nonspherical particles	Chains
23	19.0	15.7	11.3	32.8	7.2	14
30	21.6	18.5	5.7	20.9	5.0	23.2
62	30.2	13.4	3.2	39.0	1.2	13.2

4. CHEMICAL AND ELEMENTAL COMPOSITION

Rather numerous measurements of chemical and elemental composition of the volcanic aerosols are evidence of the similar processes of their generation and subsequent evolution: emission of the products of abrasion of the crater walls and particles of finely dispersed lava as well as water vapor, sulfur gas, hydrochloric acid, and volatile metals, which then take part in different chemical reactions and are condensed. Chemical analysis of smoke and dust matter of different volcanos[24] shows the predominating content of silicon compounds (60–80%), sulfates (30–10%), calcites (3–10%), aluminum compounds (0–20%), and iron (1–10%). However, more detailed consideration of the results of chemical and elemental analysis is also evidence of essential differences in the emitted matter composition for different volcanos.[25–27]

The transformation of the chemical composition of aerosol particles with the increase of altitude is characteristic of the powerful volcanic eruptions, namely, the strong enrichment of some moderately volatile elements (As, Se, Pb, Cd, and Zn) containing in small particles and the elements characteristic of magma (Si, Ca, Sc, Ti, Fe, Zn, and Th) contained in larger particles. This can be interpreted only as the fact that the sources of substances at the upper boundary of a plume are hot emissions of magma rather than the particles of the broken top of the volcano.[28] The changes of chemical and elemental composition of the volcanic substance in different periods of the eruption are also observed.[29]

When analyzing the variability of the elemental composition of the aerosols of volcanic origin, it is convenient to use the elemental content normalized to the reference matter such as elemental composition of magma, emitted lava, or ashes of different rocks. Analysis of the composition of different rocks carried out for individual eruptions is evidence of significant variations of their elemental composition, with silicon dioxide content being most constant. The following data on the silicon dioxide content in lava of volcanos of different types were reported in Ref. 30: basalt-toluate (Kilauea volcano), 47–52%; andesite (Fuego volcano), 48–54%, phonolite-tephrite, 50–55%; dacite (Saint-Helens volcano), 65–70%; and rhyolite (Ascya volcano), 68%. Variations of the content of Al are significantly greater, especially in the lavas of the dunite rock, whereas of Ca and Mg – in syenites, for which the significant losses of Fe, Na, K, Ti, Mn, Ni, and P are also observed.[31]

Variations of the elemental content in ashes are still greater. For example, the elemental analysis of the ashes after the Popocatepetl volcano eruptions (December 21, 1994–January 28, 1995) showed that the ashes are highly enriched, in comparison with the Earth's crust, by such volatile elements as S, Br, Pb, Hg, Zn, and Cu, whose enrichment factor, $FE(x) = [x]_a/[x]$, exceeds ten and varies vs. ashes emission time.

Thus, the elements should be actually normalized to the elemental composition of the Earth's crust, using Si as a reference element. In this case, the error for the majority of elements should not exceed 20–30%. The unified technique was applied to reveal the spatiotemporal variability of the elemental composition of volcanic aerosols. Tables V and VI present the values of the enrichment factors obtained from measurements of the aerosol elemental composition after the eruptions of Augustin[32] and Popocatepetl[33] volcanos.

The change of the relative contribution of elements vs. altitude is well seen from the data of Ref. 32. The increase of the enrichment factor with altitude is observed for the elements Na, K, Mn, Ba, S, V, Sc, Hf, Yb, As, Eu, W, Se, and Au and the decrease is observed for Cl, Pb, Br, and Cd.

The result is not trivial and, possibly, is evidence of more quick generation and condensation growth of particles containing Cl, Pb, Br, and Cd in comparison with the compounds containing other elements. Temporal variability of the enrichment factors of some elements is still more interesting. The values of FE for Al, K, Ba, Cl, Th, and Sm are relatively constant. The significant excess of the enrichment factor for the elements Fe, Ca, Mg, V, Cr, La, Co, and Sc was observed only during the first day, whereas the regular decrease of the enrichment factor for Ti, Mn, W, Cd, Zn, Cu, Pb and Au was observed by more than an order of magnitude for Zn, Cu, Cd, and Pb.

The behavior of the elements As, Sb, Se, and Br was similar. The high values of their enrichment factors were observed during the first day of measurements, their sharp decrease (by an order of magnitude) during the second day, and then their regular decrease. The value of FE for Br decreases 15 times during the third day. The largest emission of the volcanic substance into the atmosphere was observed on February 2. The enrichment factors for Na, Pb, Hg, and Ca increased, whereas the significant decrease of the enrichment factors for S, Mg, Cs, Rb, Cr, and Co with $FE < 1$ and for Cu, Ba, Sr, and V, with $FE < 1$ was observed. The element S is a particular case. Its FE was <1 on February 2–4 and increased up to 49 by February 21. Very low values of FE for some terrigenous elements (Fe, Al, Ca, K, Ti, Cr, Mn, Ca, and Zr) were obtained after the eruption of Popocatepetl volcano. The increase of the enrichment factor for the majority of elements was observed till January 14, 1995 with subsequent decrease of FE corresponding to the sharp decrease of the intensity of eruption.

The enrichment factor for S was quite high already at the start of measurements ($FE \sim 200$) and reached 440–600 by January 28. The strong dependence of the enrichment factor for some elements on meteorological conditions was observed: the increase of FE for S was observed during the night and morning hours and of Cu, Br, and Se – during the day hours.

Measurements of the elemental composition of aerosols after the eruption of Colima volcano in December of 1994 showed that several groups of elements can be separated according to the diurnal behavior of the enrichment factor (Fig. 9): 1) elements S, Hg, Se, Cu, Ni, Rb, Ga, Zr, and Cr, which have the well-pronounced maximum in the wee hours of the morning (3–5 a.m.); 2) Br, Y, and Cl with maximum at 9–11 p.m.; 3) P, Pb, Al, Zn, and Ti, which have the second maximum at noon obviously related to dusting from soil, in addition to the maximum at 3–5 a.m.; and, 4) Fe, Ca, Mn, K, and Sr, which have neutral diurnal behavior of FE, i.e., the same behavior as Si.

TABLE V. Enrichment factors for different elements of the atmospheric aerosols. Augustin volcano, February 1–21, 1976.

Element	February 1		February 2		February 3	February 4	February 20	February 21
	0–8 km	8–32 km	0-8 km	8–32 km	Troposphere			
Al	1.08	1.11	1.15	1.83	1.25	1.32	1.13	1.13
Fe	1.31	0.85	0.92	1.68	0.92	0.89	0.80	0.80
Ca	1.51	1.66	0.83	1.27	1.13	1.08	0.95	0.95
Na	1.18	1.43	1.61	2.70	1.74	1.74	1.2	1.2
K	0.44	0.51	0.41	0.78	0.61	0.61	0.54	0.51
Mg	1.55	0.81	0.41	0.54	0.46	0.49	0.38	–
Ti	1.51	1.43	0.83	1.08	0.75	0.63	0.68	0.54
Mn	0.98	1.43	0.94	1.59	0.97	0.91	0.86	0.77
Ba	2.2	3.2	1.67	3.4	2.6	2.2	2.3	1.92
S	1.31	3.1	0.121	0.063	0.050	0.058	49	49
Sr	< 7.6	< 3.3	0.66	2.6	1.42	0.79	–	–
Cl	7900	4100	350	5.3	20	62	–	–
V	1.46	1.75	1.13	1.31	0.94	0.95	0.84	0.84
Rb	< 0.35	0.31	0.16	0.34	0.19	0.28	–	–
Cr	<15	<13	0.167	4.2	0.132	0.166	0.120	0.144
Zn	9.4	6.4	7.4	12.	5.2	2.8	–	–
Ce	0.66	0.71	0.61	0.72	0.98	0.82	0.87	0.54
Cu	29	16	4.7	7.7	3.7	1.72	3.4	1.5
La	1.64	0.60	0.58	0.88	0.69	0.58	0.61	0.51
Co	1.0	1.07	0.55	0.99	0.52	0.55	0.45	0.50
Sc	1.45	1.64	0.92	1.66	0.95	1.03	0.82	0.93
Pb	52	23	56	24	9.6	7.9	–	–
Th	0.49	0.44	0.59	0.98	0.67	0.60	–	–
Sm	0.68	0.83	0.79	0.29	1.00	0.73	–	–
Cs	0.18	0.16	0.12	0.23	0.95	0.55	–	–
Hf	1.28	1.49	1.79	3.2	2.1	1.92	1.82	1.63
Yb	0.89	1.32	0.91	1.75	1.50	1.20	–	–
As	370	460	36	80	28	17	25	14
Eu	0.72	0.84	0.90	1.62	1.12	1.06	1.02	0.92
W	5.9	8.3	1.79	2.8	< 0.60	< 0.73	–	–
Sb	304	260	33	66	32	17	27	14
Br	38000	13000	3500	1400	197	180	–	–
Cd	290	166	65	22	39	27	35	24
Hg	> 55000	> 76000	> 56000	> 6200	< 2500	> 1500	–	–
Se	3600	4900	320	630	240	122	214	110
Au	47	96	8.5	16	6.5	5.9	6.3	5.1
M, μg /m^3	20	9.77	2100	250	620	145	–	–

TABLE VI. *Enrichment coefficients FE (x) normalized to Si for different elements contained in aerosol samples collected after the eruption of Popocatepetl volcano.*

| Element	December 29, 1994	January 6, 1995	January 14, 1995	January 21, 1995	January 27, 1995	January 27−28, 1995	January 28, 1995
Fe	0.24	0.228	0.72	0.36	0.40	0.40	0.32
Al	1.04	1.20	1.64	1.36	1.12	1.24	1.60
Ca	0.48	0.52	0.84	0.68	0.68	0.72	0.72
S	1.92	340	432	364	180	592	436
P	≤ 4.4	< 7.2	21.2	≤ 7.6	≤ 4.8	≤ 6.0	6.8
Cl	28.8	44	144	100	26.4	52	68
K	0.16	0.20	0.20	0.12	0.32	0.28	0.28
Ti	0.36	0.24	0.48	0.52	0.48	0.48	0.44
Cr	0.72	0.44	3.00	2.16	0.60	1.24	0.76
Mn	0.12	0.22	0.60	0.15	0.27	0.32	0.24
Ni	0.37	0.33	2.24	0.80	0.56	0.92	0.80
Cu	8.4	2.08	18.0	3.16	0.96	1.36	2.40
Zn	1.12	0.64	7.2	2.32	1.56	2.64	2.44
Ga	0.23	0.19	2.44	1.56	0.52	≤ 0.44	1.20
Se	13.6	18.0	104	28	6.4	11.8	44
Br	10.4	12.4	48	19.8	22.4	12.8	9.2
Rb	0.18	0.22	2.16	1.32	0.48	0.64	1.08
Sr	0.40	0.40	0.44	0.92	0.56	0.68	0.44
Y	≤ 0.54	1.08	≤ 296	3.44	≤ 0.72	≤ 1.20	3.52
Zn	≤ 0.34	0.27	1.52	0.72	0.72	0.72	0.52
Hg	≤ 180	≤ 260	≤ 740	≤ 360	≤ 180	≤ 240	≤ 330
Pb	5.2	7.6	36	13.6	7.2	12.8	11.6
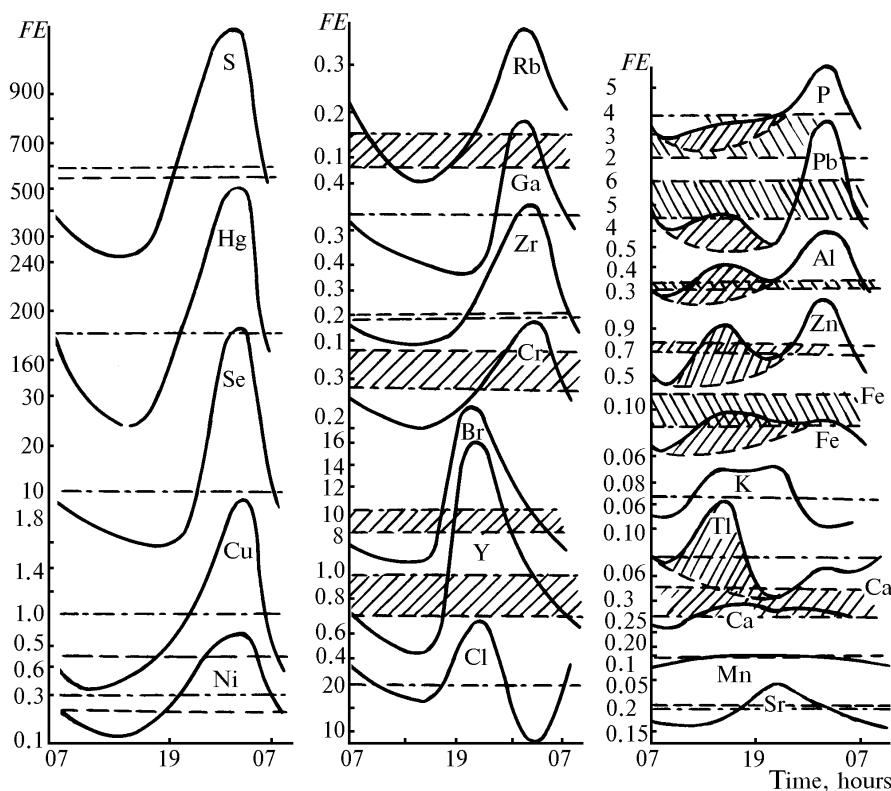
FIG. 9. *Diurnal behavior of the enrichment factors for different elements (Colima, December of 1994).*
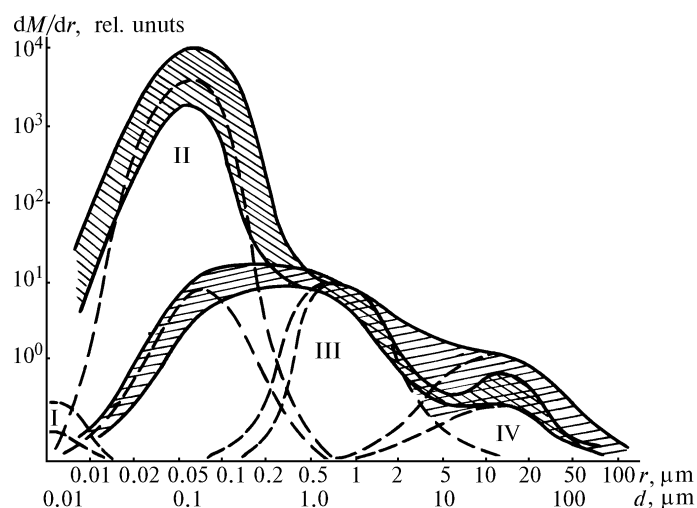
FIG. 10. *Mass distribution of aerosols of natural origin for different elements (Pamir, Glacier Fedchenko; Alma-Ata, Astrophysical Institute): − − − Br, Cr and Zn (principal contribution to fraction II); - - Na, Cu, Sm, and Hg (principal contribution to fraction III); ——— Fe, Sc, Au, Sb, Ti, and Pb (fractions III and IV).*

Attempts to establish the features in the behavior of different elements contained in the volcanic matter were undertaken in Refs. 34−36. In particular, the enrichment factor of the volcanic aerosols was shown to be dependent on the size of particles that contain the element under investigation, as well as on the ambient conditions of measurements. However, the data on the enrichment factors obtained for different volcanos (15 eruptions) and on the dependence of the enrichment factor for element X on the size of particles containing this element were characterized by too wide spread of the values for the majority of elements.

The renormalization of the data on the enrichment factors to the Earth's crust composition by the unified technique showed that the data essentially ordered when classified into three groups: far from the source (airborne and ground−based measurements), near the lava flow, and over fumaroles and in fumarole fields.

The physically understandable regularities of variation of $FE(x)$ are revealed from such a classification: the dependence of $FE(x)$ on the temperature and the source strength (the depth from which the volcanic substance is emitted) as well as on the meteorological conditions, i.e., on the conditions of aerosol accumulation in the layer where measurements were carried out.

We have already investigated the elemental composition of different fractions of the aerosols of natural origin by means of a cascade impactor with three-layer filters (Fig. 10). Some similarity with the distribution of elements contained in the volcanic aerosols was revealed. It is very important that the significant number of elements is distributed over two and even three modal fractions, but not in one. The fraction by weight of these modes can vary essentially (depending on the temperature of sublimation of substance and the lifetime of a particle). This should obviously affect the enrichment factor variations.

5. OPTICAL PROPERTIES OF VOLCANIC DUST

A lot of observations of spatiotemporal structure of aerosol optical thickness of the atmosphere have been carried out in the visible wavelength range after powerful volcanic eruptions to date.[37−40] Aerosol optical thickness of the cloudless atmosphere varied from 0.05 to several units, depending on the distance from the source. Second and sometimes third maximums of τ_a were often observed after the first one in the clear atmosphere. These maximums exceeded the first one and were primarily caused by chemical transformation of gaseous products of the volcanic emission (sulfur gas) into aerosols (sulfuric acid and sulfates).[41]

The majority of spectral measurements of solar radiation extinction by the volcanic aerosols were related to the cases in which the contribution of sulfuric acid and sulfate aerosols to the extinction of radiation was principal.

However, at the initial stage of eruption, especially for eruptions when the volcanic matter does not reach the stratosphere, the contribution of the dust matter (primordial volcanic aerosols) is more significant. In this case, the maximum of the aerosol optical thickness can be observed in its spectral behavior in the wavelength range[42] 500−700 nm (Fig. 11). Possibly, it is responsible for the anomalous spectral behavior of the radiation extinction in the atmosphere. We note that it is often observed in dry air masses[43] and for the high transparency of the atmosphere in the ground layer.[44]

The results of calculations of the spectral coefficients of aerosol extinction for three characteristic cases of distribution of dust particles of volcanic origin in the wavelength range 300−1000 nm shown in Fig. 12

confirm the possibility of the anomalous spectral behavior of the aerosol extinction. The calculations were done for two constant refractive indices $n = 1.65$ and 1.50 and for different maximum size of particles $d_1 = 1.0$ μm, $d_2 = 2.0$ μm, and $d_3 = 15$ μm.
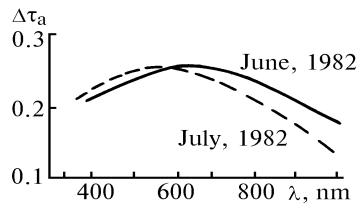
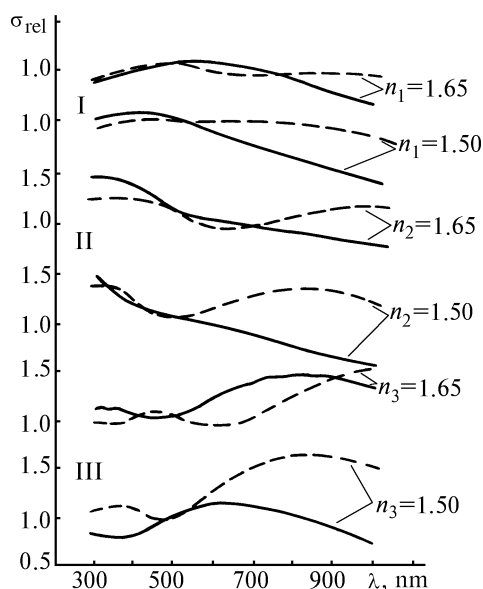FIG. 11. *Residual optical thickness six months after the eruption of El Chichon volcano (data of De Luisi et al[42]).*

FIG. 12. *Results of calculation of the relative spectral behavior of the aerosol extinction coefficients of volcanic dust for $r_{max} = 0.5$ μm, $r''_{max} = 1.0$ μm, and $r'''_{max} = 15$ μm. The distribution functions correspond to the data of Table II.*

The anomalous spectral behavior manifests itself after removal of the bulk of giant particles from the atmosphere. It can occur in the period from some days to some months depending on the altitude of the dust matter plume.

It should be noted that the results of calculations of the aerosol extinction coefficients for the refractive index $n_2 = 1.50$ correspond better to the results of direct spectral observations. It can be caused, in particular, by using the results of measurements by the photoelectric counter for model calculations, because the counter is calibrated by the latex particles with the refractive index $n = 1.50$. This may distort the true curve of the particle size distribution slightly shifting it toward larger particles. In addition,

measurements with a finer gradation of particle size are necessary in the range $0.8 \leq d \leq 2.0$ μm. However, this does not radically change the results obtained.

6. CONCLUSION

The analysis of the experimental investigations of microstructure, chemical and elemental composition, and optical properties of the aerosols near some volcanos with different intensities of emission of the dispersed substance carried out under different meteorological conditions has shown that, in spite of significant variety of the characteristics obtained, some peculiarities and similarity of these characteristics are observed for the volcanic aerosols. The most important peculiarities making them different from the aerosols of another origin, are the following:

1) Two characteristic maximums are observed in the size spectrum of particles of volcanic origin for small intensity of the eruption. They are in the ranges $0.6 \leq d \leq 1.0$ μm and $2.0 \leq d \leq 4.0$ μm.

2) Morphological structure of the primordial aerosol particles of volcanic origin (dust) principally corresponds to the type of particles of disperse origin. A portion of sulfuric acid and sulfate particles near the volcano increases only for long emission of sulfur gas.

Relative humidity of air affects significantly the morphological structure of particles.

3) Elemental composition of the dust fraction of volcanic aerosols is characterized by obvious enrichment by volatile elements such as Zn, Cu, As, Sb, Hg, and Pb, as well as by noticeable enrichment by elements characteristic of aerosols of condensation (chemical and photochemical) origin: S, Se, and Cl.

The relative content of different elements contained in the aerosols is determined by the type of emission of the volcanic substance (energy of explosion, temperature, duration of the eruption), distance from the source, and meteorological conditions under which the samples were collected.

4) The primordial volcanic aerosols can be responsible for the anomalous spectral behavior of the aerosol optical thickness of the atmosphere.

ACKNOWLEDGMENTS

REFERENCES

1. *M.L. Asaturov, M.I. Budyko, K.Ya. Vinnikov, et al., Volcanos, Stratospheric Aerosols, and Earth's Climate (Gidrometeoizdat, Leningrad, 1986), 256 pp.*

2. K.Ya. Kondrat'ev, ed., *Aerosol and Climate* (Gidrometeoizdat, Leningrad, 1991).

3. L.S. Ivlev, V.M. Zhukov, V.I. Kudryashov, and E.F. Mikhailov, Atmos. Oceanic Opt. **6**, No. 10, 715–726 (1993).

4. J.J. Michalsky, E.W. Pearson, and B.A. Le Baron, J. Geophys. Res. **95**, No. D5, 5677–5688 (1990).

5. D.V. Michelangeli, M. Allen, and Y.L. Yung, J. Geophys. Res. **94**, No. D15, 18429–18443 (1989).

6. K.Ya. Kondrat'ev, N.I. Moskalenko, and D.V. Pozdnyakov, *Atmospheric Aerosol* (Gidrometeoizdat, Leningrad, 1983), 224 pp.

7. V.E. Zuev and G.M. Krekov, *Optical Models of the Atmosphere* (Gidrometeoizdat, Leningrad, 1986), 256 pp.

8. G.M. Krekov and R.F. Rakhimov, *Optical Radar Model of Continental Aerosol* (Nauka, Novosibirsk, 1982), 198 pp.

9. L.L. Basov, L.S. Ivlev, V.G. Sirota, and S.P. Smyshlyaev, Zh. Ekol. Khimii, No. 1, 77–86 (1992).

10. M.R. Schoeberl, P.K. Bhartia, E. Kilsenrath and O. Torres, Geophys. Res. Let. **20**, No. 1, 29–32 (1993).

11. R.L. Chuan, J. Palais, W.J. Rose, et al., J. Atmos. Chem., No. 4, 467–477 (1986).

12. L.S. Ivlev, G.A. Karpov, A.A. Kist, et al., Vulkanologiya Seismologiya, No. 1, 32–42 (1986).

13. R.G. Knollenberg and D. Huffman, Geophys. Res. Lett., No. 10, 1020–1028 (1983).

14. L.S. Ivlev, J. Galindo, and V.I. Kudryashov, Internat. Geophys. (in print) (1996).

15. L.S. Ivlev, V.A. Ionin, A.Yu. Semova, and N.K. Spazhakina, Trudy Gl. Geofiz. Obs., No. 293, 161–172 (1972).

16. S.J. Lane, J.S. Gilbert, and M. Hilton, Bull. Volcanol. **55**, 481–488 (1993).

17. W.A. Sedlacek, E.J. Mroz, A.L. Lazrus, and B.W. Gandrud., J. Geophys. Res. **88**, 3741–3776 (1983).

18. R.L. Chuan, D.G. Woods, and M.P. McCormik, Science **211**, 830–832 (1983).

19. J. Heintzenberg, Tellus **41B**, No. 2, 149–160 (1989).

20. A. Deepak and J.P. Box, in: *Atmos. Aerosol*, (1982), pp. 79–110.

21. F. Kasten, J. Appl. Meteorol. **7**, No. 5, 944–947 (1968).

22. L.S. Ivlev, in: *Problems of Atmospheric Physics*, Vol. 14 (1978), pp. 89–96.

23. L.S. Ivlev, *Chemical Composition and Structure of Atmospheric Aerosols* (Leningrad State University Publishing House, Leningrad, 1982), 366 pp.

24. S. Rasool, ed., *Chemistry of the Lower Atmosphere* (Plenum Press, New-York–London, 1973).

25. A.Z. Mikleshanskii, Yu.V. Yakovlev, I.A. Menyailov, et al., Geokhimiya, No. 11, 1652–1661 (1975).

26. T.K. Hinkley, Bull. Volcanol. **53**, 395–400 (1991).

27. P. Buat-Menard and M. Arnold, Geophys. Res. Lett. **5**, No. 4, 387–392 (1978).

28. R.B. Symonds, M.H. Reed, and W.J. Rose, Geochim. Cosmochim. Acta **56**, No. 5, 633–672 (1992).

29. T.K. Hinkley, M.F. Le Cloarec, and G. Lambert, Geochim. Cosmochim. Acta **58**, No. 15, 3255–3263 (1994).

30. M.P. Rampino and S. Self, Quart. Res. **18**, 127–143 (1982).

31. *Handbook on Geochemistry* (Nedra, Moscow, 1982), 184 pp.

32. E.A. Lepel, K.M. Stefansson, and W.H. Zoller, J. Geophys. Res. **83**, No. C12, 6213–6220 (1978).

33. L.S. Ivlev and J. Galindo, in: *Proceedings of the 11th Aerosol Conference*, Pittsburg (1995).

34. H. Tazieeff and J.C. Sabroux, eds., *Forecasting Volcanic Events* (Elsevier, Amsterdam, 1983), 584 pp.

35. J.P. Quisefit, G. Bergametti, R. Vie La Sage, and F.C.R. Le Guern, Acad. Sci. Paris **293**, 325–328 (1981).

36. G. Lambert, M.F. Le Cloarec, and M. Pennisi, Geochim. Cosmochim. Acta **52**, 39–42 (1988).

37. W.G. Egan, Appl. Opt. **23**, No. 7, 1013–1020 (1984).

38. J.E. Hay and R. Darbu, Atmosphere–Ocean **22**, No. 3, 354–368 (1984).

39. J.A. Davies, R. Schroeder, and L.J.B. McArthur, Tellus **40B**, 154–160 (1988).

40. M. Amman and H. Burtscher, J. Geophys. Res. **98**, No. B11, 19705–19711 (1993).

41. L.S. Ivlev, V.G. Sirota, and S.N. Khvorostovskii, Atm. Opt. **3**, No. 1, 30–36 (1990).

42. J.J. De Luisi, E.G. Dutton, C.L. Coulson, et al., J. Geophys. Res. **88**, No. C11, 6769–6772 (1983).

43. S.I. Avdyushin, E.E. Artemkin, V.I. Emel'yanov, and A.E. Mikirov, in: *Problems of Atmospheric Optics*. Tr. Inst. Prikl. Geofiz., No. 40 (1980), pp. 65–73.

44. S.F. Rodionov, *Electrophysical Investigations of the Atmosphere over Mt. El'brus* (Gidrometeoizdat, Leningrad, 1970), 125 pp.